City, University of London Institutional Repository

This is the accepted version of the paper.

This version of the publication may differ from the final published version.

Permanent repository link: https://openaccess.city.ac.uk/id/eprint/27320/

Link to published version: http://dx.doi.org/10.1109/EMBC46164.2021.9630319

Recurrent Neural Network Models for Blood Pressure Monitoring Using PPG Morphological Features

Chadi El Hajj and Panayiotis A. Kyriacou

Abstract— Continuous blood pressure monitoring is vital for the early detection and control of hypertension. However, this is unreachable using current non-invasive and cuff-based devices. Several methods have been proposed to overcome this challenge, one of the most attractive ones is the photoplethysmography approach. Although, good performance has been reported in the literature, it was mainly achieved on small inadequate sample size using conventional models that are unable to account for the temporal variations in the input vector. To address these limitations, this paper proposes cuffless and continuous blood pressure estimation using Long Short-term Memory (LSTM) and Gated Recurrent Units (GRU). The models were evaluated on 942 patients acquired from the Multiparameter Intelligent Monitoring in Intensive Care dataset. The proposed models produced superior results in comparison with conventional artificial neural network. In particular, the best performance was achieved by the GRU, with mean absolute error and standard deviation of 5.77±8.52 mmHg and 3.33±5.02 mmHg for systolic and diastolic blood pressure, respectively.

I. INTRODUCTION

Blood pressure (BP) is a vital sign and quite an important indicator of the health condition of a person. In particular, BP measurement is used for monitoring the cardiovascular functions of the body. High blood pressure poses several health risks with potentially fatal consequences. Early stages of high blood pressure (hypertension) often do not display any symptoms, hence patients are unaware of their health condition until later stages [1]. For this reason, it is known as the silent killer and could lead to life-threatening diseases such as renal dysfunction and cardiovascular diseases (CVDs) [2]. Therefore, continuous BP monitoring is important for the early detection, diagnosis and treatment of hypertension as well as CVD.

In clinical practice, the most common non-invasive BP measurement devices are the sphygmomanometers [3]. These devices are widely considered as the gold standard and the most accurate for BP monitoring. However, despite their merits, there are few disadvantages to these devices. Most notably, they require a cuff wrapped around the arm for determining the BP values. Additionally, proper training is needed to operate as improper cuff-size (inadequate inflation and compression) may lead to false reading. Furthermore, these devices do not provide continuous BP measurements. Therefore, it is difficult to track the changes of BP over time. Hence, the cuff-based approaches are not suitable and inconvenient for accurate diagnosis and control of hypertension.

Chadi El Hajj and Panayiotis A. Kyriacou are with the Research Centre for Biomedical Engineering, at City, University of London, Northampton Square, London EC1V 0HB, United Kingdom {Chadi.El-Hajj,p.Kyriacou}@city.ac.uk

There have been numerous attempts for developing cuffless and non-invasive BP methods. Pulse Wave Velocity (PWV) is a popular approach that has been studied in the literature [4]. PWV is the propagation speed of the pressure wave in the vessels. BP measurement using this method is based on the fact that an increase in BP reflects an increase in PWV. Pulse transit time (PTT) is commonly used to estimate PWV [5], [6], [8]. It is defined is the time that takes the pressure wave to propagate between arterial sites. An inverse correlation is often found between PTT and BP. PTT is measured as the time between the peak of the electrocardiogram (ECG) signal and a particular point on the photoplethysmogram (PPG) signal. While good performance have been reported for BP estimation using the PTT method, it was mainly achieved on a relatively small dataset. Additionally, there are considerable disadvantages to this approach such as the need for two measurement sensors, and the accurate PTT estimation is dependent on the synchronisation of the two signals. This is highly demanding in practice and makes the PTT approach inconvenient for continuous BP measurement.

Recently, a new approach has been investigated by many researchers that is based on PPG pulse wave analysis [9], [11], [13], [14]. Unlike the PTT approach, this method relies only on PPG signals without the ECG, thus a single device is needed for measurement. Additionally, the PPG sensor is a low-cost, simple, and cuff-less sensor, as opposed to the ECG sensor where several electrodes have to be directly attached to the body. The PPG approach is predominately based on extracting temporal features from the PPG waveform cycles. Subsequently, the relationship between the PPG and BP is explicitly modelled using machine learning and neural network models. For examples, Teng and Zhang [9] established a linear regression model using four PPG features, namely, systolic upstroke time, diastolic time and width at 50 and 66 % amplitude. The results were promising, however, the model was evaluated on a small number of healthy subjects. Khalid et al [14] presented a comparison study between several linear and non-linear machine learning models including support vector machine and regression tree. The regression tree outperforms the linear model and support vector machine. Kurylyak et al [11] extracted 21 time domain features and employed an artificial neural network (ANN) for estimating SBP and DBP. The performance of the ANN was reasonable, however, it was evaluated on a small dataset. Sadrawi et al [12] used the raw PPG signals for estimating the arterial BP waveform using a genetic based deep convolution auto-encoder. These studies reported varying

results which were highly dependent on the dataset used (e.g. demographics, health conditions and number of subjects) as well as features and models employed. Generally, non-linear models, particularly neural networks, performed reasonably well, paving the way for a new cuffless and continuous BP estimation methods.

Considering that the previously mentioned methods can estimate BP cufflessly, they do not explicitly model the time dependency in the PPG features that had been proven to further enhance the precision in BP estimation [5], [8]. In order to overcome this drawback, in this paper, we employ recurrent neural networks, namely, LSTM and GRU to account for the variations in the PPG features with respect time whilst estimating BP.

The rest of the paper is organised as follows. Section II introduces the dataset, pre-processing steps, PPG features and three neural network models. Section III demonstrates the experimental results and section IV concludes the paper.

II. METHODOLOGY

A. Dataset description

The signals used in this paper were originally collected from the Multiparameter Intelligent Monitoring in Intensive Care (MIMIC II) [15]. The dataset provides several important signals such as PPG, ECG, invasive BP etc, collected from thousands of patients in intensive care units (ICU). All signals were recorded simultaneously at 125 Hz sampling frequency. Since the signals collected from the MIMIC II contains several deteriorated and unreliable segments, we used a pre-processed dataset published by Kachuee et al [6]. This dataset contains clean and pre-processed PPG and ECG signals as well as reference to arterial BP (ABP) signals, extracted from 942 patients from the MIMIC II. The range of SBP and DBP values in the final dataset are shown in Fig. 1
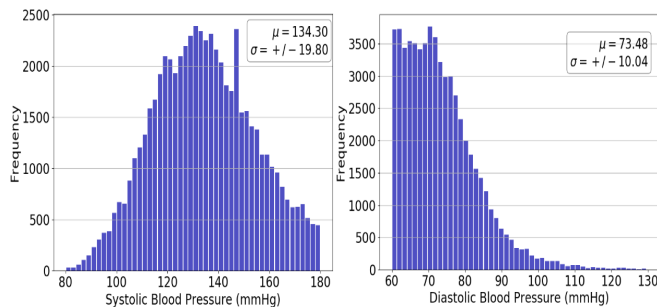

Fig. 1: SBP and DBP range in the final dataset

B. Data pre-processing

In the PPG approach, signal pre-processing is an important step in order to accurately extract useful features from the waveform. Also, it is crucial during pre-processing to avoid oversmoothing the signals as certain meaningful features might be lost while others become harder to detect. Fortunately, the obtained signals [6] were efficiently pre-processed while preserving as much information as possible.

Hence, some pre-processing steps follow the same procedure described in [6]. The pre-processing steps include:

- A simple averaging filter was performed on the signals and highly deteriorated segments were removed as described in [6], [7]
- Very High and very low BP values were removed (SBP $\geq$ 180, SBP $\leq$ 80, DBP $\geq$ 130, DBP $\leq$ 60)
- The PPG signal was normalised using min-max normalisation

The result of the pre-processing steps is a clean PPG signal free from baseline wandering. Afterwards, the PPG and their reference BP signals were divided into 10 s segments from which the features described in the following section are extracted. Finally, the dataset was partitioned into 70% train, 15% validation and 15% test sets.

C. Feature extraction

In this paper, we originally extracted 52 time domain features from the PPG and first and second derivatives. Previous studies have successfully established a relationship between these features and BP which was modelled using using linear and non-linear data driven models. The reported results demonstrate that the non-linear models outperform the linear models [6], [7], [11], particularly on large datasets with signals collected from varying demographics including sick patients, such as the MIMIC II.

The extracted PPG features mainly describe useful characteristics of the pulsatile component of the waveform, such as amplitudes and duration. For examples, Teng and Zhang [9] extracted width at 1/2 and 2/3 amplitude as well systolic uptroke time (ST) and diastolic time (DT). In [10] width at 10% amplitude, cardiac period and pulse height were investigated. Other studies build upon these findings by adding more features that captures the PPG morphology more accurately. In [11], the number of features were increased to 21 temporal features, by adding pulse width at 25%, 33%, and 75% amplitude from both systolic and diastolic phase. An additional 14 features were added in [13] from the second derivative of the PPG. In this study, we considered several more features from the PPG such as pulse area which was used in [14], ratio of pulse interval to peak amplitude, PPG peak etc., as well as features from the first derivative and second derivative.

In order to further increase the overall performance of the model, in terms of the trade off between the accuracy and complexity, we apply several feature selection methods to eliminate redundant features and reduce the dimension of the input vector. In order to select the most significant features, the following steps were taken:

- First, Pearson's Correlation Coefficient between every pair of features were analysed to identify pairs with very strong linear relationship (i.e. colinear features)
- Second, Maximal Information Coefficient (MIC) was applied to assess the importance of each feature on the target output
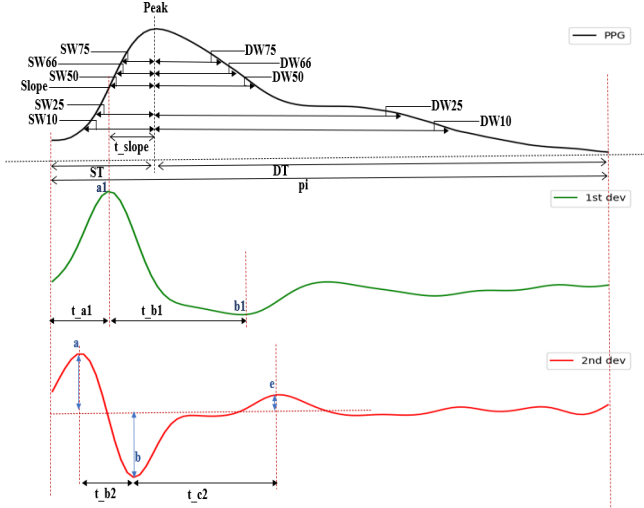
Fig. 2: Time domain features from the PPG (black) and its first (green) and second derivatives (red)

- Third, the feature with the highest MIC value between the pair of colinear features was kept while the other was eliminated
- Fourth, Recursive Feature Elimination (RFE) was applied on the obtained feature vector, from the previous step, to select the features with the highest influence on BP by considering their impact on the performance of a fitted random forest model. As a result, the least effective features on the estimation were dropped.

Following the above mentioned steps, the input vector was reduced to 24 features. These features were then normalised to suppress the effect of outliers in the dataset. The selected features are presented in Table I and shown in Fig. 2

TABLE I: Feature definition

Feature	Definition
1. PPG Peak	Systolic peak of the PPG waveform
2. Systolic time (ST)	Time interval from the beginning of the PPG waveform to its peak
3. Diastolic time (DT)	Time interval from the peak of the PPG to the end of the waveform
4. t_slope/pi	Ratio of the time between the rising slope and peak of PPG (t_slope) to pulse interval (pi)
5. pi/peak	Ratio of pulse interval to the peak of the PPG
6. DW10	Diastolic width at 10 % amplitude
7. DW10/SW10	Ratio of diastolic width to systolic width at 10 % amplitude
8. DW25	Diastolic width at 25 % amplitude of the waveform
9. DW25/SW25	Ratio of diastolic width to systolic width at 25 % amplitude
10. DW50	Diastolic width at 50 % amplitude of the PPG waveform
11. DW50/SW50	Ratio of diastolic width to systolic width at 50 % amplitude
12. DW66/SW66	Ratio of diastolic width to systolic width at 66 % amplitude
13. DW75+SW75	Width of the PPG waveform at 75 % amplitude
14. t_a1	Time interval from the beginning of the waveform to the peak (a1) of the first derivative
15. t_b1	Time interval from the peak (a1) to the first valley (b1) of the first derivative
16. t_a1/pi	Ratio of t_a1 to pulse interval pi
17. t_b1/pi	Ratio of t_b1 to pulse interval pi
18. b	Valley intensity of the second derivative of the PPG
19. b/a	Ratio of the first valley to first peak (a) of the second derivative of the PPG
20. e/a	Ratio of the second peak (e) to the first peak of the second derivative of the PPG
21. t_b2	Time interval from first peak to the first valley of the second derivative of the PPG
22. t_c2	Time interval from the first valley to second peak of the second derivative of the PPG
23. t_b2/pi	Ratio of t_b2 to pulse interval pi
24. t_c2/pi	Ratio of t_c2 to pulse interval pi

D. Neural network models

As mentioned previously, comparative analysis evaluated on well representative dataset had proven that there is a non-linear relationship between the PPG and BP [6], [7], [11], [14]. Additionally, previous studies have also shown that the estimation accuracy can be further improved by taking into consideration the temporal variations in the PPG signal [5], [8]. For these reasons, we consider two different approaches using non-linear models. In the first approach, we apply an ANN as a non-recurrent baseline model, while in the second approach we employ recurrent models (LSTM and GRU) which consider the time dependencies in the PPG features for the estimation. The following describes the neural network models:

- ANN: is a feedforward neural network where adjacent units in one layer are fully connected with the units in the next layer forming an acyclic graph (non-recurrent connections). The non-linear activation function of the hidden units is the Rectified Linear Units (ReLu). Several combinations of hidden layers, learning rates and hidden units were tested during the experiments. The best performance was achieved using 0.01 learning rate, and three hidden layers with 100, 250 and 500 units, respectively.
- LSTM: is a variant of recurrent neural networks (RNN) that is able to effectively handle the long and short term dependencies in the data while solving the vanishing gradient problem in deep learning models. After finetuning the model parameters, the optimised model consists of four hidden layers with 512 units in each layer and the learning rate is 0.0001.
- GRU: is another variant of RNN, and simpler version of the LSTM. It was also established to efficiently model time series data but with less parameters to tune compared to the LSTM. The optimised model consists of three hidden layers with 512 units in each layer and the learning rate is 0.001.

The cost function for all these models was the mean squared error. The optimiser used for training is Adam optimiser with backpropagation.

III. RESULTS

The results from the optimised models are presented in Table II. The performance was assessed using the mean absolute error (MAE) and standard deviation (SD) on the test set. The experimental results show that the performance of the LSTM and GRU were superior compared to the non-recurrent ANN model. This proves that modelling the time dependencies in the PPG can enhance the model performance. It is also evident from Table II that the GRU produced slightly better results than the LSTM for the SBP and comparable performance for the DBP. Fig. 3 presents further analysis of the results obtained by the GRU, which was considered as the best model. The histograms show that the estimation error for SBP and DBP fall within $\pm$ 10 mmHg and $\pm$ 5 mmHg, respectively. Furthermore, the correlation

plots demonstrate a very strong relationship between the estimated and reference values.

(a) Histograms of error differences

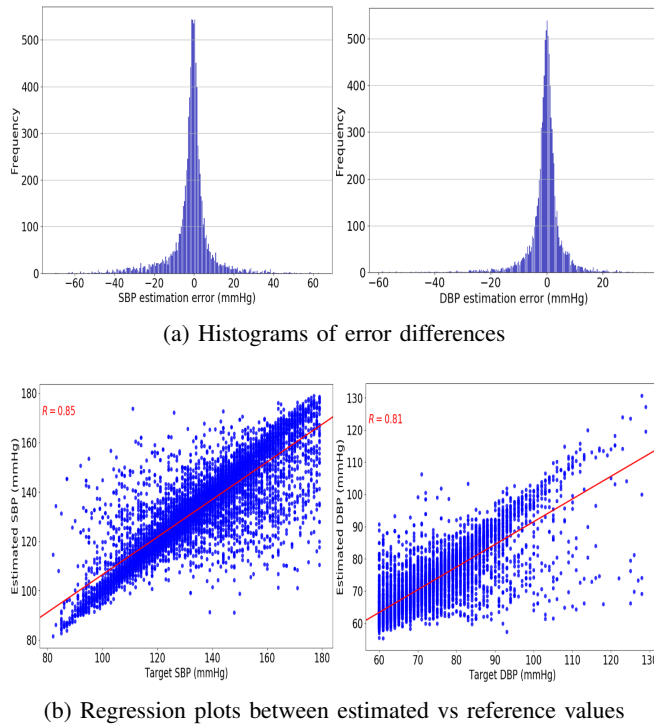(b) Regression plots between estimated vs reference values

Fig. 3: GRU estimation analysis vs ground-truth values for SBP (left) and DBP (right) using: (a) error histograms, (b) correlation plots with regression line

TABLE II: Performance results of different BP methods

Algorithms	SBP		DBP	
	MAE (mmHg)	± SD (mmHg)	MAE (mmHg)	± SD (mmHg)
ANN	9.21	8.84	5.16	5.41
LSTM	5.97	8.81	3.27	4.99
GRU	**5.77**	**8.52**	**3.33**	**5.02**

Table III presents the performance of the GRU compared to the Association for the Advancement of Medical Instrumentation (AAMI) standards. The AAMI requires the mean error (ME) and SD to be below 5 ± 8 mmHg evaluated on at least 85 subjects [16]. It can be seen in Table III that the GRU performance for the DBP estimation is within the required range, however, fell short of the SD requirement for the SBP estimation.

TABLE III: Performance against the AAMI standard

		ME (mmHg)	SD (mmHg)	Subjects
AAMI	SBP and DBP	≤ 5	≤ 8	≥ 85
GRU	SBP	-1.24	10.21	942
	DBP	-0.44	5.7	942

IV. CONCLUSION

This paper proposes methods for cuff-less and continuous SBP and DBP estimation from a single optical sensor, namely, PPG. Various time domain features were extracted from its morphology as well as the first two derivatives. Through feature analysis, colinear and redundant features were removed from the feature vector, effectively reducing size of the input by more than half. Subsequently, two recurrent models were employed to estimate BP and their results were compared with a simple ANN. The best performance was achieved using the GRU model, and DBP estimation satisfies the AAMI standards, while the SD for the SBP was slightly higher than the accepted margin.

REFERENCES

[1] World Health Organization, 2013. A global brief on hypertension: silent killer, global public health crisis: World Health Day 2013 (No. WHO/DCO/WHD/2013.2). World Health Organization.
[2] He, J. and Whelton, P.K., 1999. Elevated systolic blood pressure and risk of cardiovascular and renal disease: overview of evidence from observational epidemiologic studies and randomized controlled trials. American heart journal, 138(3), pp.S211-S219.
[3] Ogedegbe, G. and Pickering, T., 2010. Principles and techniques of blood pressure measurement. Cardiology clinics, 28(4), pp.571-586.
[4] Gribbin, B., Steptoe, A. and Sleight, P., 1976. Pulse wave velocity as a measure of blood pressure change. Psychophysiology, 13(1), pp.86-90.
[5] Tanveer, M.S. and Hasan, M.K., 2019. Cuffless blood pressure estimation from electrocardiogram and photoplethysmogram using waveform based ANN-LSTM network. Biomedical Signal Processing and Control, 51, pp.382-392.
[6] Kachuee, M., Kiani, M.M., Mohammadzade, H. and Shabany, M., 2015, May. Cuff-less high-accuracy calibration-free blood pressure estimation using pulse transit time. In 2015 IEEE international symposium on circuits and systems (ISCAS) (pp. 1006-1009). IEEE.
[7] Kachuee, M., Kiani, M.M., Mohammadzade, H. and Shabany, M., 2016. Cuffless blood pressure estimation algorithms for continuous health-care monitoring. IEEE Transactions on Biomedical Engineering, 64(4), pp.859-869.
[8] Su, P., Ding, X.R., Zhang, Y.T., Liu, J., Miao, F. and Zhao, N., 2018, March. Long-term blood pressure prediction with deep recurrent neural networks. In 2018 IEEE EMBS International Conference on Biomedical & Health Informatics (BHI) (pp. 323-328). IEEE.
[9] Teng, X.F. and Zhang, Y.T., 2003, September. Continuous and non-invasive estimation of arterial blood pressure using a photoplethysmographic approach. In Proceedings of the 25th Annual International Conference of the IEEE Engineering in Medicine and Biology Society (IEEE Cat. No. 03CH37439) (Vol. 4, pp. 3153-3156). IEEE.
[10] Linder, S.P., Wendelken, S.M., Wei, E. and McGrath, S.P., 2006. Using the morphology of photoplethysmogram peaks to detect changes in posture. Journal of clinical monitoring and computing, 20(3), pp.151-158.
[11] Kurylyak, Y., Lamonaca, F. and Grimaldi, D., 2013, May. A Neural Network-based method for continuous blood pressure estimation from a PPG signal. In 2013 IEEE International instrumentation and measurement technology conference (I2MTC) (pp. 280-283). IEEE.
[12] Sadrawi, M., Lin, Y.T., Lin, C.H., Mathunjwa, B., Fan, S.Z., Abbod, M.F. and Shieh, J.S., 2020. Genetic Deep Convolutional Autoencoder Applied for Generative Continuous Arterial Blood Pressure via Photoplethysmography. Sensors, 20(14), p.3829.
[13] Liu, M., Po, L.M. and Fu, H., 2017. Cuffless blood pressure estimation based on photoplethysmography signal and its second derivative. International Journal of Computer Theory and Engineering, 9(3), p.202.
[14] Khalid, S.G., Zhang, J., Chen, F. and Zheng, D., 2018. Blood pressure estimation using photoplethysmography only: comparison between different machine learning approaches. Journal of healthcare engineering, 2018.
[15] Goldberger, A.L., Amaral, L.A., Glass, L., Hausdorff, J.M., Ivanov, P.C., Mark, R.G., Mietus, J.E., Moody, G.B., Peng, C.K. and Stanley, H.E., 2000. PhysioBank, PhysioToolkit, and PhysioNet: components of a new research resource for complex physiologic signals. circulation, 101(23), pp.e215-e220.
[16] Association for the Advancement of Medical Instrumentation, 1987. American national standards for electronic or automated sphygmomanometers. ANSI/AAMI SP 10-1987.